Multicolor nonreciprocal optical amplifier with spinning active optomechanics

Ru-Ting Sun,[1] Mei-Yu Peng,[1] Tian-Xiang Lu,[2,*] Jie Wang,[1] Qian Zhang,[1] Ya-Feng Jiao,[3,4,†] and Hui Jing[1,4,‡]

[1]*Key Laboratory of Low-Dimensional Quantum Structures and Quantum Control of Ministry of Education, Department of Physics and Synergetic Innovation Center for Quantum Effects and Applications, Hunan Normal University, Changsha 410081, China*

[2]*College of Physics and Electronic Information, Gannan Normal University, Ganzhou 341000, Jiangxi, China*

[3]*School of Electronics and Information, Zhengzhou University of Light Industry, Zhengzhou 450001, China*

[4]*Academy for Quantum Science and Technology, Zhengzhou University of Light Industry, Zhengzhou 450001, China*

(Received 12 October 2023; accepted 31 January 2024; published 20 February 2024)

We propose to achieve a multicolor nonreciprocal optical amplifier, a crucial device in optical communication and information processing, by spinning an active resonator. We show that in such a device, due to the interplay of the Sagnac effect and the optical gain, nonreciprocal signal amplification can be realized, accompanied by a giant enhancement of optical group delay from 0.3 ms to 35 ms in a chosen direction, which is otherwise unattainable in a passive device. Also, coherent amplification of higher-order optical sidebands and a slow-to-fast light switch can be achieved by tuning both the pump power and the spinning velocity. Our work provides a unique and accessible way, well compatible with other existing techniques, to realize multicolor nonreciprocal optical amplifiers for more flexible control of optical fields.

DOI: 10.1103/PhysRevA.109.023520

I. INTRODUCTION

Nonreciprocal optical devices, featuring distinct properties of light transmission when interchanging the ports of input and output, are indispensable for backscattering-immune optical communications [1–3], optical cloaking [4,5], and quantum information processing [6–13]. Recently, rapid advances have been witnessed in achieving on-chip nonreciprocal devices without any magnetic material, based on space-time modulations [14–16], nonlinear and chiral interactions [9,17–28], or non-Hermitian structures [29–32]. In a very recent experiment, 99.6% optical isolation was achieved by spinning a resonator at 6.6 kHz [33]. This provides a versatile platform to explore more possibilities such as nonreciprocal solitons or chaos [34,35], nonreciprocal sensing [36,37], and nonreciprocal control of quantum correlations [38–47]. In practice, multicolor nonreciprocities are indeed of interest, making it possible to realize one-way transmissions or communications at different frequencies with a single device [48–51]. However, as far as we know, it has not yet been revealed how to achieve multicolor nonreciprocal amplification with such a spinning device, integrated also with an ability to enhance and switch the optical delay or advance.

In parallel, we note that active optical resonators containing gain materials [52–60] can radically change optical features or light-matter interactions, thus leading to different effects in such a non-Hermitian system [61–64]—for instance, fast light [65], inverted optical transparency [62,66,67], topological lasing [68], parity-time symmetry breaking [61,69–72], and optical nonreciprocity [31,72–74]. Also, in the context of cavity optomechanics (COM), gain-enhanced light-motion couplings have enabled findings such as thresholdless phonon lasing [61,69,75], surface-emitting lasing [76,77], and enhanced COM sensing [78]. Inspired by these works, we propose to realize a nonreciprocal multicolor optical amplifier by spinning an active COM resonator.

Specifically, we consider a spinning COM resonator coupled to a tapered fiber and study the roles of both optical gain and mechanical rotations in the process of optomechanically induced transparency (OMIT). We show that in this system, multicolor nonreciprocal signal amplification can be realized by tuning the spinning velocity of the resonator, also with well-tunable effects of the nonreciprocal group delay or advance. In addition, nonreciprocal amplification can be realized for higher-order optical sidebands emerging in such an active COM system, indicating the possibility to achieve a nonreciprocal amplifier with a single resonator.

The paper is organized as follows. In Sec. II, we introduce our model of an active spinning COM system and quantify the optical transmissions. Detailed discussions of the generation and manipulation of the nonreciprocal lights, including those for the probe signal transmission, group delay, and higher-order sidebands, are shown in Sec. III, and a summary is given in Sec. IV.

II. THEORETICAL MODEL

As shown in Fig. 1(a), we consider a spinning whispering-gallery mode resonator with frequency ω_c and the optical intrinsic decay rate $\gamma_c = \omega_c/Q$ (with Q being the optical quality factor). This resonator supports a mechanical radial breathing mode (with frequency ω_m and effective mass m) that is coupled to the optical mode via optical-radiation-pressure

*lu.tianxiang@foxmail.com
†yfjiao91@foxmail.com
‡jinghui73@foxmail.com

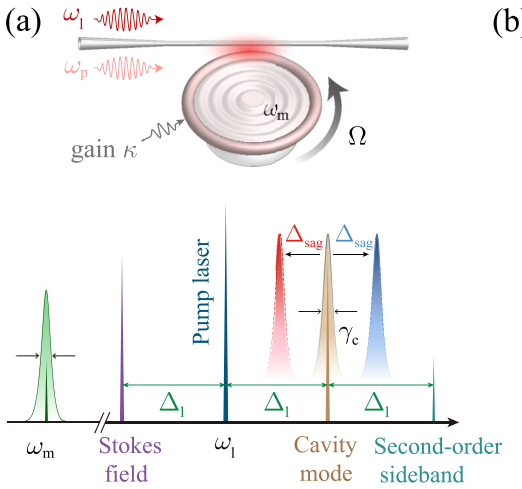

(b)

Parameter	Symbol	Value [79]
Optical resonance frequency	ω_c	194 THz
Pump power	P_l	10 W
Mechanical mode frequency	ω_m	200 MHz
Mechanical damping rate	Γ_m	0.2 MHz
Effective mass of mechanical mode	m	2 μg
Refractive index of the resonator	n	1.44
Radius of the resonator	R	0.25 mm
The optical quality factor	Q	3×10^7
Total optical loss	γ	6.43 MHz
COM coupling	$g=\omega_c/R$	772 PHz

FIG. 1. (a) Schematic diagram and frequency spectrum of an active resonator that spins along the counterclockwise direction with an angular velocity Ω. The resonator can support a mechanical mode of frequency ω_m and is driven by a strong pump laser at frequency ω_l and a weak probe laser at frequency ω_p. Therefore, we have $\Delta_{sag} > 0$ or $\Delta_{sag} < 0$ for the case with the driving field (including pump laser and probe laser) on the left-hand or right-hand side. (b) Summary of experimentally accessible parameters for numerical simulations [79].

induced interaction. To explore the OMIT effect, a strong pump laser is applied at frequency ω_l and a weak probe laser at frequency ω_p to drive the system, with the field amplitudes

$$\varepsilon_l = \sqrt{\gamma_{ex} P_l/\hbar\omega_l}, \quad \varepsilon_p = \sqrt{\gamma_{ex} P_s/\hbar\omega_p},$$

respectively, with P_l (P_s) the input power of the pump (probe) laser and γ_{ex} the external decay rate of resonator-fiber coupling [80,81]. Hereafter, we denote the total optical loss rate by $\gamma = (\gamma_c + \gamma_{ex})/2$.

Our aim here is to study how to manipulate the OMIT effect by combining the roles of the Sagnac effect and the gain. We note that in experiments, the active resonator can be fabricated by using gain materials [31,32], such as a silica microtoroid doped with Er^{3+} ions, which can emit photons in the 1550-nm band when driven by a laser in the 980-nm or 1450-nm band [31]. The effective gain of the cavity can be achieved using the coherent perfect absorption of the two input fields fed into the cavity [82,83] or the intracavity optical parametric amplifier [84,85]. Also, very recently, the rotary resonator was realized by mounting on a turbine spinning along its axis [33]. For the resonator with radius R and angular velocity Ω, the frequency of the optical mode undergoes an opposite Sagac-Fizeau frequency shift [86–91], i.e., $\omega_c \to \omega_c + \Delta_{sag}$, with

$$\Delta_{sag} = \pm\Omega\frac{nR\omega_c}{c}\left(1 - \frac{1}{n^2} - \frac{\lambda}{n}\frac{dn}{d\lambda}\right), \tag{1}$$

where n is the refractive index of the resonator and c (λ) is the speed (wavelength) of light in vacuum. The dispersion term $dn/d\lambda$, describing the relativistic origin of the Sagnac effect, is relatively small in typical materials (reaching up to $\sim$1%) [33,86]. Fixing the counterclockwise rotation of the resonator, we have $\Delta_{sag} > 0$ ($\Delta_{sag} < 0$) for the case with the driving field (including pump laser and probe laser) input from the left-hand (right-hand) side.

The effective Hamiltonian of the system, in a frame rotating at driving frequency ω_l, can be written as

$$\begin{aligned} H =& \hbar(\Delta_l + \Delta_{sag})a^\dagger a + \frac{p^2}{2m} + \frac{1}{2}m\omega_m^2 x^2 + \frac{p_\theta^2}{2mR^2} \\ & - \hbar g a^\dagger a x + i\hbar(\varepsilon_l a^\dagger + \varepsilon_p a^\dagger e^{-i\xi t} - \text{H.c.}), \end{aligned} \tag{2}$$

where $\Delta_l = \omega_c - \omega_l$, $\xi = \omega_p - \omega_l$, and $g = \omega_c/R$ denotes the COM coupling rate. a ($a^\dagger$) is the optical annihilation (creation) operator, and x, p, θ, and p_θ are displacement, momentum, rotation angle, and angular momentum operators, respectively, which satisfy the commutation relations $[x, p] = [\theta, p_\theta] = i\hbar$ [92].

The mean response of the system to the probe signal, rather than including quantum fluctuation, is processed by OMIT in COM systems [80,81]. As a result, for the sake of exploring the nonlinear dynamics of it, the equations of motion of the system can be derived as

$$\begin{aligned} \dot{a} &= [-i(\Delta_l + \Delta_{sag}) + \kappa + igx]a + \varepsilon_l + \varepsilon_p e^{-i\xi t}, \\ \ddot{x} &= -\omega_m^2 x + \frac{\hbar g}{m}a^\dagger a - \Gamma_m \dot{x} + \frac{p_\theta^2}{m^2R^3}, \\ \dot{\theta} &= \frac{p_\theta}{mR^2}, \quad \dot{p}_\theta = 0, \end{aligned} \tag{3}$$

where $\Omega = \dot{\theta}$ is the speed of rotation. Note that the optical or mechanical damping terms are added phenomenologically into the above equation. In the following, we have assumed that for $\kappa/\gamma = -1$, κ denotes the optical decay, whereas for $\kappa/\gamma = 1$, κ denotes the optical gain. Moreover, for $\kappa/\gamma = 0$, the system becomes a lossless one with zero net gain (i.e., the real gain we introduced equals the loss).

All the deductions are based on small signal approximation, which requires the use of strong pump light and weak probe light, under which the probe can be regarded as the perturbation of the steady states [80,81]. The pump field supplies

the steady-state solution of the dynamical variables

$$a_s = \frac{\varepsilon_l}{i\Delta - \kappa}, \quad x_s = \frac{\hbar g}{m\omega_m^2}|a_s|^2 + R\left(\frac{\Omega}{\omega_m}\right)^2, \tag{4}$$

where $\Delta = \Delta_l + \Delta_{sag} - gx_s$ is the effective optical detuning. Obviously, the steady-state mechanical displacement x_s and the intracavity optical amplitude a_s are determined by the angular velocity Ω and the optical gain κ. As a result, the effective COM coupling rate and the breathing mode oscillations of the active spinning COM system can be tuned by adjusting the rotating speed and the gain-to-loss ratio, which in turn leads to the modified OMIT properties of the system. Physically, the centrifugal force caused by rotation provides an additional drive to the mechanical vibration, causing a change in the equilibrium position of the dynamic vibration [92].

For the scenario where the probe light for OMIT process is generally much weaker than the pump light [93], every operator can be expanded as a sum of its steady-state mean value and small fluctuations around that value, that is,

$$x = x_s + \delta x, \quad a = a_s + \delta a. \tag{5}$$

After the steady-state value is eliminated, the perturbations caused by the input probe field satisfy the following equations [80,81]:

$$\begin{aligned}\delta\dot{a} &= (-i\Delta + \kappa)\delta a + ig(a_s\delta x + \delta a\delta x) + \varepsilon_p e^{-i\xi t},\\ \delta\ddot{x} &= -\omega_m^2\delta x - \Gamma_m\delta\dot{x} + \frac{\hbar g}{m}(a_s\delta a^\dagger + a_s^*\delta a + \delta a^\dagger\delta a).\end{aligned} \tag{6}$$

To calculate the amplitudes of the first- and second-order sidebands, we solve these equations by using the ansatz [81]

$$\begin{aligned}\delta x &= X_{(1)}e^{-i\xi t} + X_{(1)}^* e^{i\xi t} + X_{(2)}e^{-2i\xi t} + X_{(2)}^* e^{2i\xi t},\\ \delta a &= A_{(1)}^+ e^{-i\xi t} + A_{(1)}^- e^{i\xi t} + A_{(2)}^+ e^{-2i\xi t} + A_{(2)}^- e^{2i\xi t},\end{aligned} \tag{7}$$

where the plus and minus signs correspond to the upper and lower sidebands [94]. By substituting Eq. (7) into Eq. (6) and neglecting the second-order parts, the linear response of the system can be obtained as

$$\begin{aligned}A_{(1)}^+ &= \frac{\varepsilon_p[\lambda_-(\xi)\nu(\xi) + i\hbar g^2|a_s|^2]}{\lambda_+(\xi)\lambda_-(\xi)\nu(\xi) - 2\hbar\Delta g^2|a_s|^2},\\ X_{(1)} &= \frac{\lambda_-(\xi)\hbar g a_s^*\varepsilon_p}{\lambda_+(\xi)\lambda_-(\xi)\nu(\xi) - 2\hbar\Delta g^2|a_s|^2},\end{aligned} \tag{8}$$

where

$$\nu(\xi) = m\left(-\xi^2 + \omega_m^2 - i\xi\Gamma_m\right), \quad \lambda_\pm(\xi) = -i\xi - \kappa \pm i\Delta.$$

By combining Eqs. (6)–(8), the second-order sideband amplitude is given by

$$A_{(2)}^+ = \frac{C_1 X_{(1)}^2 + C_2 A_{(1)}^+ X_{(1)}}{\lambda_-(\xi)C_3}, \tag{9}$$

where

$$\begin{aligned}C_1 &= -i\hbar g^4|a_s|^2 a_s,\\ C_2 &= ig\lambda_-(\xi)\nu(2\xi)\lambda_-(2\xi) - i\hbar\xi g^3|a_s|^2,\\ C_3 &= \nu(2\xi)\lambda_+(2\xi)\lambda_-(2\xi) - 2\hbar\Delta g^2|a_s|^2.\end{aligned}$$

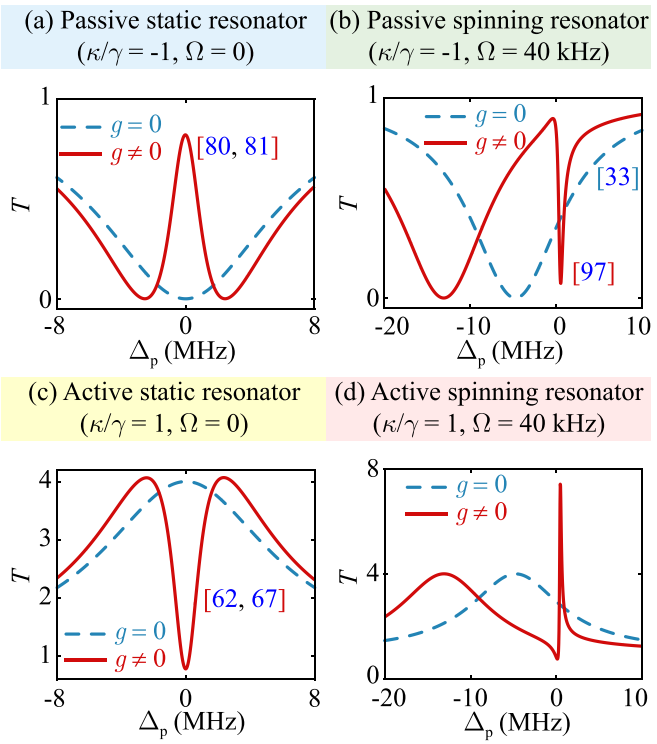

FIG. 2. Transmission rate T of the probe field as a function of the probe detuning $\Delta_p = \omega_p - \omega_c$ with or without COM coupling (i.e., $g = 0$ or $g \neq 0$) in the (a) passive static resonator [80,81], (b) passive spinning resonator [33,97], active static resonator (c) [62,67], and (d) active spinning resonator, respectively. κ/γ, Ω, and g represent the gain-to-loss ratio, rotating speed, and optomechanical coupling rate, respectively. The parameters are selected as listed in Fig. 1(b).

Using the standard input-output relation [95] $a_{out} = a_{in} - \sqrt{\gamma_{ex}}a$, the transmission rate of the probe light [62] and the efficiency of the second-order upper sideband [67] will be obtained as

$$\begin{aligned}T = |t_p|^2 &= \left|\frac{a_{out}}{a_{in}}\right|^2 = \left|1 - \frac{\gamma_{ex}}{\varepsilon_p}A_{(1)}^+\right|^2,\\ \eta &= \left|\frac{\gamma_{ex}}{\varepsilon_p}A_{(2)}^+\right|.\end{aligned} \tag{10}$$

In our numerical simulations, the experimentally accessible parameters are chosen, as shown in Fig. 1(b). According to a very related experiment [33], a spherical cavity with a radius of 1.1 mm can steadily revolve around its axis at a speed of 6.6 kHz. Theoretically, if the driving power is certain, the maximum speed is inversely proportional to the square of the radius; this means that the smaller the cavity, the greater the speed [96]. Taking these factors into account, we use a rotary speed of no more than 40 kHz.

III. RESULTS AND DISCUSSION

A. The transmission rate of the probe field

Figure 2 shows that there are obvious differences in transmission spectra with or without optomechanical coupling (i.e., $g = 0$ or $g \neq 0$). For a passive stationary resonator

[see Fig. 2(a)], when $g = 0$, the transmission spectra has a minimum at the resonance point, which is different from the standard OMIT with a transparency window where $g \neq 0$ [80,81]. When the passive resonator rotates [see Fig. 2(b)], for $g = 0$, there is only a frequency shift of the absorption spectra due to the Sagnac effect, which has been demonstrated in a recent experiment [33], and for $g \neq 0$, a Fano-like OMIT spectrum appears [97]. For an active stationary resonator [see Fig. 2(c)], when $g = 0$, the transmission spectra has a maximum at the resonance point, which is different from the inverted-OMIT with a transmission dip and two sideband peaks in the case of $g \neq 0$ [62,67]. In particular, for $g \neq 0$, a Fano-like inverted-OMIT profile occurs in the case of an active spinning resonator [see Fig. 2(d)], accompanied by highly asymmetric amplification due to the interplay of the Sagnac effect and the optical gain. Therefore, we explore nonreciprocal amplification with an active spinning optomechanical resonator.

For comparison, we first consider the case of a static resonator. Figure 3(a) shows the transmission rate T of the probe field versus detuning Δ_p for different values of the gain-to-loss ratio κ/γ. In the standard COM system (i.e., a passive static COM resonator), a standard single transparency window emerges around the resonance point [81] [see the green dashed curve in Fig. 3(a)]. This is also consistent with the description in Refs. [62,67], where when the amount of gain provided to the resonator supersedes its loss, and the resonator becomes an active resonator, an inverted-OMIT profile appears for the probe field [see the red solid curve in Fig. 3(a)], which can be viewed as an analog of the optical inverted electromagnetically induced transparency (EIT) [66]. In addition, we have also confirmed that in a spinning COM system without any gain, the nonreciprocal transmission of light can be achieved, which is reminiscent of the result discussed in Ref. [97]. Figure 3(b) shows the transmission rate T of the probe field versus optical probe detuning Δ_p for different input directions in the passive spinning resonator. For a fixed rotary direction, the probe light coming from the left or the right can be blocked or transmitted due to the rotation-induced Sagnac frequency shift, leading to the emergence of nonreciprocal light propagation [97].

Inspired by these preceding works, we now study how to achieve a nonreciprocal optical amplifier with an active spinning optomechanical resonator. In Figs. 3(c)–3(e), we depict the effect of rotation on the signal transmission rate in an active COM system. It is worth noting that, in the presence of rotation, a wider OMIT linewidth can be obtained by increasing the spinning speed, resulting in a Fano-like inverted-OMIT transparency spectrum [see Fig. 3(c)]. In particular, the amplification of the nonreciprocal signal is easily obtained by tuning the directions of the input probe field, and the nonreciprocal isolation can be as high as 6 dB by selecting the appropriate speed and detuning [see Fig. 3(d)], which is caused by the interplay of the Sagnac effect and the optical gain. This essential physics can be understood as follows: as shown in Refs. [62,67], increasing the gain can turn a conventional OMIT profile into an inverted-OMIT profile. Meanwhile, the rotation of the resonator increases the amplitude of the steady-state mechanical displacement explosively. For example, when choosing $\Omega = 40$ kHz, x_s can be increased

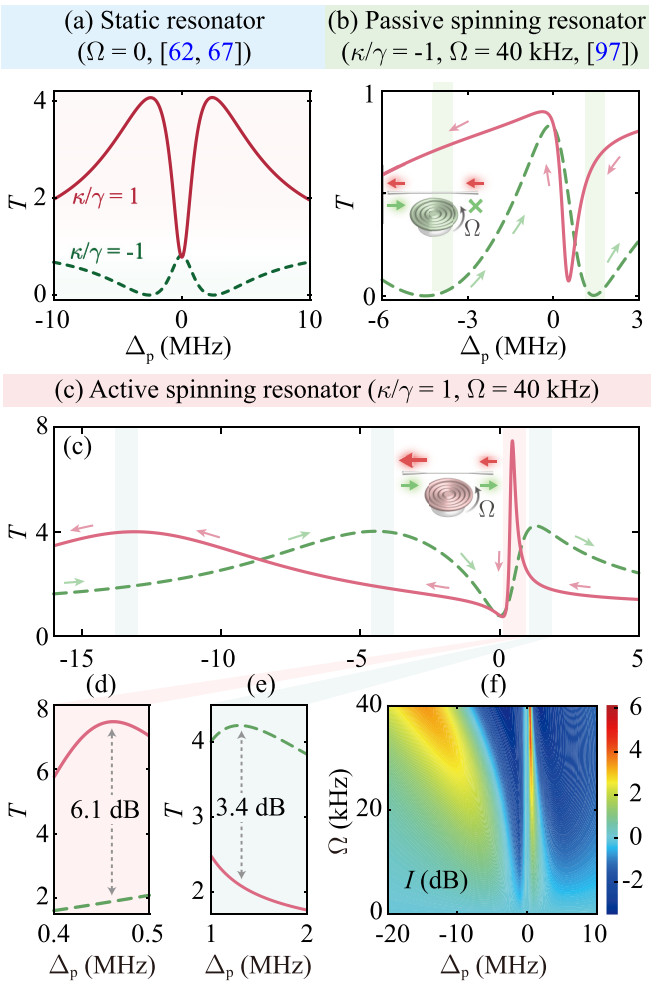

FIG. 3. (a) Inverted OMIT [62,67]: Transmission rate T of the probe field as a function of the detuning Δ_p for different values of the gain-to-loss ratio κ/γ in a static resonator. (b) Nonreciprocal transmission [97]: T vs Δ_p for different input directions in a passive spinning resonator. Arrows represent input on the left-hand or right-hand side, and green bands correspond to regions with strong nonreciprocity. Inset: Schematic diagram of a passive resonator spins along the counterclockwise direction. The probe light coming from the left or the right can be blocked (the green fork) or transmitted (the red arrow), leading to nonreciprocal light propagation. (c)–(e) Nonreciprocal amplification: T vs Δ_p for different input directions in an active spinning resonator. (f) Isolation ratio I vs Δ_p and the rotating speed Ω in the active resonator. The parameters are selected as listed in Fig. 1(b).

from 80 fm to 10 pm, thus leading to a strong enhancement of the effective COM coupling rate $G = gx_s$ [97]. Hence, when Ω and Δ_p are kept fixed, a nonreciprocal optical amplifier can be realized due to the interplay between the Sagnac effect and gain materials. Moreover, the multicolor nonreciprocal light amplification is observed by tuning the directions of the input driving field [see Figs. 3(c)–3(e)].

Depending on the direction of the input driving field, the transmittance of the probe field exhibits a highly asymmetric feature because the optical frequency shift caused by rotation is related to the driving direction [97]. In order to better understand and visualize the effect, we define the isolation

ratio as [37]

$$I = 10\log_{10}\frac{T_{\leftarrow}}{T_{\rightarrow}}. \tag{11}$$

Fixing the counterclockwise rotation of the resonator, $T_{\rightarrow}$ ($T_{\leftarrow}$) denotes the driving field input from the left-hand (right-hand) side. Figure 3(f) shows that the isolation ratio I depends on the optical detuning Δ_p for different values of the rotary speed Ω to give a comprehensive view.

The maximum value of isolation I increases with a higher rotary speed in the active resonator. This implies that, by transforming Δ_p and Ω, the gain of light with direction dependence can be controlled to achieve a unique nonreciprocal feature. It is obvious that the nonreciprocal amplification effect will be further enhanced, if we can continue to increase the speed of the active cavity.

B. Optical group delay

Accompanied with the OMIT, slowing or advancing of light can also be observed [62,80,81]. Specifically, the group delay of the probe light is given by

$$\tau = \left.\frac{d\arg(t_p)}{d\xi}\right|_{\xi=\omega_m}. \tag{12}$$

To see this, we plot the group delay of the probe light τ as a function of the driving power P_l for different values of gain-to-loss ratio κ/γ in Fig. 4.

We find that the dispersion of the spinning active resonator can be severely affected by the interplay of the Sagnac effect and the optical gain [62,67,97], resulting in the rotary speed and the driving direction becoming the two control knobs to regulate the group delay. For a passive spinning resonator, we have confirmed that OMIT leads only to the slowing of the transmitted light [97]. In contrast, in a static active resonator (i.e., $\kappa/\gamma = 1$ and $\Omega = 0$), one can tune the system to switch from slow to fast light, or vice versa, by tuning the driving power P_l [62,67]. Moreover, the group delay τ can also be significantly enhanced by about 40 times for their maximum values in comparison with the passive static resonator [62,67]. In particular, by spinning the active resonator (i.e., $\kappa/\gamma = 1$ and $\Omega \neq 0$), nonreciprocal group delay or advance can be realized [see Fig. 4(b)]. More importantly, in an active spinning resonator, the group delay τ can be further significantly enhanced for the case with the driving field input from the right-hand side [see Figs. 4(b) and 4(d)]. For example, the maximum value of the group delay τ is about 35 ms for $\Omega = 3$ kHz, i.e., about 111 times enhancement compared to that for $\Omega = 0$.

C. Nonlinear second-order sideband

We note that nonlinear OMIT effects, usually exhibiting as weak signals of higher-order optical sidebands, can arise due to nonlinear COM interactions [98–101]. The possibility of amplifying these weak signals has been explored in very recent works [67,93,102–105], with a static active cavity or coupled resonators [67], a nonlinear Kerr resonator [102], a parity-time symmetric system consisting of a passive nonlinear cavity coupled to an active linear cavity [103], a

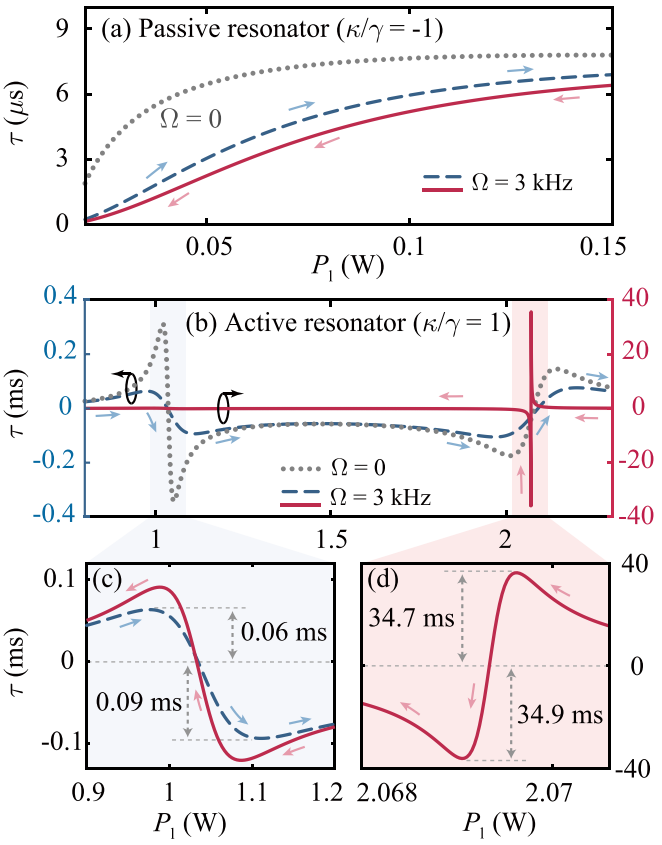

FIG. 4. Group delay τ of the probe light as a function of the pump power P_l for different input directions in (a) a passive COM resonator or (b)–(d) an active COM resonator. Arrows correspond to input on the left-hand or right-hand side. Here, $\Omega = 3$ kHz for the spinning resonator, and $\Omega = 0$ for the nonspinning resonator. As marked by the black circle and arrow, both the gray dotted curve and blue dashed curve correspond to the left axis, and the red solid curve corresponds to the right axis. For the other parameter values, see the table in Fig. 1(b).

mechanically pumped COM system [104], and a magnomechanical system [93]. Also, nonreciprocal enhancement of such sidebands can also be achieved by considering a spinning passive resonator [106,107] or a nonlinear optomagnonic system [108]. Here, we show that well-controllable nonreciprocal amplifications of nonlinear OMIT effects can be realized in our present system.

To verify the role of optical gain and mechanical rotation in enhancing the second-order sideband in our system, we plot Figs. 5(a)–5(c) to demonstrate that the efficiency η varies with the optical detuning Δ_p. For a passive static resonator ($\Omega = 0$ and $\kappa/\gamma = -1$), the second-order sideband is subdued when the OMIT emerges [98], which results in a local minimum between the two sideband peaks around $\Delta_p = 0$ [see the green dashed curve in Fig. 5(a)]. As we know from Ref. [67], in an active static resonator, the double-peak spectrum still exists and η is enhanced by the gain [see the red solid curve in Fig. 5(a)]. However, in a spinning COM system without any gain, the nonreciprocal enhancement of the second-order sideband can be achieved, which is reminiscent of the result discussed in Ref. [107]. As shown in Fig. 5(b), when

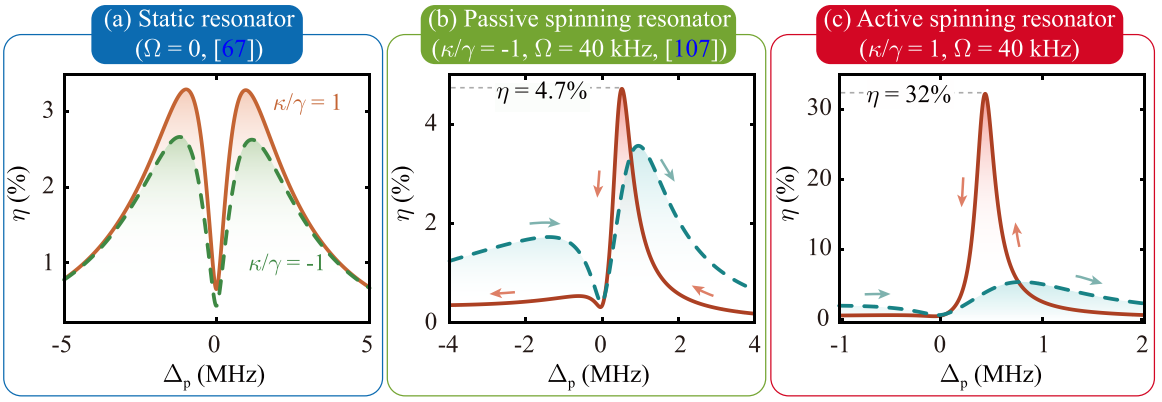

FIG. 5. (a) The efficiency η of the second-order sideband as a function of the optical detuning Δ_p for different values of the gain-to-loss ratio κ/γ in the static resonator [67]. η vs Δ_p for different input directions in (b) the passive resonator [107] or (c) the active resonator. Arrows correspond to input on the left or right side. The parameters are selected as listed in Fig. 1(b).

driving the system from the right-hand side, the left peak is completely suppressed and the right peak is only marginally enhanced compared to driving the system from the left-hand side. This result means that, by rotating the resonator, nonreciprocal enhancement of the second-order sideband can be achieved in a passive resonator due to the Sagnac effect [107].

More interestingly, for an active device, the second-order sideband can be further enhanced dramatically compared to the passive device. For example, when driving the system from the right-hand side, the efficiency η is about 32% for $\kappa/\gamma = 1$ [see the red solid curve in Fig. 5(c)], i.e., about seven times enhancement compared to that for $\kappa/\gamma = -1$. The reason for the phenomenon is that the interplay of the Sagnac effect and the gain results in the left peak of the second-order sideband being completely suppressed while the right peak is considerably enhanced.

D. Experimental feasibility

In our work, the effects of backscattering, rotation on the stable coupling of fiber with the cavity, the Kerr nonlinear effect, and the thermal nonlinear effect are not considered for the following reasons:

(1) Backscattering: For the quality factor $Q = 3 \times 10^7$, the recent experiment on spinning resonator already confirmed that the backscattering is negligible [33]. In addition, even in the presence of strong backscattering, we have shown in our previous works that in a nonreciprocal device as in our system, backscattering effect can be directionally suppressed in a specific direction, thus even benefiting the appearance of nonreciprocal effects [38,39].

(2) The self-adjustment mechanism: According to recent experiments [33], for such a device with high-speed rotating single cavity coupling a fiber, the aerodynamic process plays a key role in stabilizing resonator-waveguide coupling—a rapidly rotating resonator can drag air into the area between the taper and the cavity, thus forming the air border layer. Because of the air pressure on the surface of the taper facing the resonator, it flies above the cavity at a height that can reach several nanometers. If some disturbance causes the taper to rise above the stable equilibrium height, it will float back to its original position. Through this self-adjustment process, a stable coupling between the resonator and the fiber taper is maintained [33]. Other factors, such as intermolecular forces, lubricant compressibility, tapered-fiber stiffness, and the wrap angle of the fiber, may affect the resonator-fiber coupling. However, these factors have been proven to be negligible in the experiment [33]. Therefore, we believe that the fiber can be stably coupled to the high-speed rotating single cavity.

(3) The Kerr nonlinear effect and the thermal nonlinear effect: Indeed, these nonlinearities can lead to frequency shifts in the OMIT spectrum, but as shown in a recent experiment, such shifts can be compensated for by changing the optical detuning of the driving laser [109]. The thermal effects can be further weakened by, e.g., cooling the device in a low-temperature environment [81] or coupling with an auxiliary high-Q cavity [110]. The interesting possibility of achieving nonreciprocal amplification in our present system even without any compensation (via, e.g., choosing different detuning regimes) will be explored in detail in our future works.

IV. CONCLUSIONS

Nonreciprocal effects of rotation have been extensively studied, such as nonreciprocal light transmission by rotating a pure optical resonator [33], nonreciprocal transmission [97], and nonreciprocal enhancement of second-order sideband [107] based on COM systems, but none of these works involves gain. Similarly, researchers have also paid attention to the phenomena such as inverted OMIT, second-order sideband amplification, and the corresponding slow light effects caused by the gain in COM systems [62,67].

In our work, we have theoretically studied how to achieve a multicolor nonreciprocal optical amplifier by spinning an active COM resonator. We find that in such an active spinning COM system, the optical Sagnac effect and the optical gain strongly impact the optical properties, including the signal transmission and its higher-order sidebands. As a result, nonreciprocal signal amplification can be realized, accompanied by a giant enhancement of the optical group delay from 0.3 ms to 35 ms in a chosen direction, which is useful for optical storage. Moreover, nonrecip-

rocal enhancement of the second-order sideband can be further enhanced supernormally compared to the passive spinning resonator. These features of nonreciprocal optical amplification and giant enhancement of the optical group delay provide more flexible ways in practical applications ranging from multicolor optical communications to optical storage. Our work can also be extended to study enhancement of sensing—for instance, nanoparticle sensing [36,111], the gyroscope [112], and nonreciprocal topological photonics [113].

ACKNOWLEDGMENTS

H.J. is supported by the National Natural Science Foundation of China (NSFC, Grants No. 11935006 and No. 11774086), the Hunan Provincial Major Sci-Tech Program (Grant No. 2023ZJ1010) and the Science and Technology Innovation Program of Hunan Province (Grant No. 2020RC4047). T.-X.L. is supported by the NSFC (Grant No. 12205054) and the Ph.D. Research Foundation (Grant No. BSJJ202122). Y.-F.J. is supported by the NSFC (Grant No. 12147156).

[1] A. D. Kim and M. Moscoso, Backscattering of circularly polarized pulses, Opt. Lett. **27**, 1589 (2002).

[2] K. Fang, J. Luo, A. Metelmann, M. H. Matheny, F. Marquardt, A. A. Clerk, and O. Painter, Generalized non-reciprocity in an optomechanical circuit via synthetic magnetism and reservoir engineering, Nat. Phys. **13**, 465 (2017).

[3] S. Pucher, C. Liedl, S. Jin, A. Rauschenbeutel, and P. Schneeweiss, Atomic spin-controlled non-reciprocal Raman amplification of fibre-guided light, Nat. Photonics **16**, 380 (2022).

[4] T. Han, X. Bai, J. T. Thong, B. Li, and C.-W. Qiu, Full control and manipulation of heat signatures: Cloaking, camouflage and thermal metamaterials, Adv. Mater. **26**, 1731 (2014).

[5] M. Dehmollaian, G. Lavigne, and C. Caloz, Transmittable nonreciprocal cloaking, Phys. Rev. Appl. **19**, 014051 (2023).

[6] A. Sheikh Ansari, A. K. Iyer, and B. Gholipour, Asymmetric transmission in nanophotonics, Nanophotonics (2023).

[7] M. Scheucher, A. Hilico, E. Will, J. Volz, and A. Rauschenbeutel, Quantum optical circulator controlled by a single chirally coupled atom, Science **354**, 1577 (2016).

[8] M.-X. Dong, K.-Y. Xia, W.-H. Zhang, Y.-C. Yu, Y.-H. Ye, E.-Z. Li, L. Zeng, D.-S. Ding, B.-S. Shi, G.-C. Guo *et al.*, All-optical reversible single-photon isolation at room temperature, Sci. Adv. **7**, eabe8924 (2021).

[9] S. Zhang, Y. Hu, G. Lin, Y. Niu, K. Xia, J. Gong, and S. Gong, Thermal-motion-induced non-reciprocal quantum optical system, Nat. Photonics **12**, 744 (2018).

[10] L. Tang, J. Tang, and K. Xia, Chiral quantum optics and optical nonreciprocity based on susceptibility-momentum locking, Adv. Quantum Technol. **5**, 2200014 (2022).

[11] L. Tang, J. Tang, M. Chen, F. Nori, M. Xiao, and K. Xia, Quantum squeezing induced optical nonreciprocity, Phys. Rev. Lett. **128**, 083604 (2022).

[12] K. Xia, G. Lu, G. Lin, Y. Cheng, Y. Niu, S. Gong, and J. Twamley, Reversible nonmagnetic single-photon isolation using unbalanced quantum coupling, Phys. Rev. A **90**, 043802 (2014).

[13] X. Lu, W. Cao, W. Yi, H. Shen, and Y. Xiao, Nonreciprocity and quantum correlations of light transport in hot atoms via reservoir engineering, Phys. Rev. Lett. **126**, 223603 (2021).

[14] D. L. Sounas and A. Alù, Non-reciprocal photonics based on time modulation, Nat. Photonics **11**, 774 (2017).

[15] E. Li, B. J. Eggleton, K. Fang, and S. Fan, Photonic Aharonov-Bohm effect in photon-phonon interactions, Nat. Commun. **5**, 3225 (2014).

[16] L. D. Tzuang, K. Fang, P. Nussenzveig, S. Fan, and M. Lipson, Non-reciprocal phase shift induced by an effective magnetic flux for light, Nat. Photonics **8**, 701 (2014).

[17] J. Qie, C. Wang, and L. Yang, Chirality induced nonreciprocity in a nonlinear optical microresonator, Laser Photonics Rev. **17** 2200717 (2023).

[18] L. Fan, J. Wang, L. T. Varghese, H. Shen, B. Niu, Y. Xuan, A. M. Weiner, and M. Qi, An all-silicon passive optical diode, Science **335**, 447 (2012).

[19] Y. Sang, J. Xu, K. Liu, W. Chen, Y. Xiao, Z. Zhu, N. Liu, and J. Zhang, Spatial nonreciprocal transmission and optical bistability based on millimeter-scale suspended metasurface, Adv. Opt. Mater. **10**, 2201523 (2022).

[20] C. Sayrin, C. Junge, R. Mitsch, B. Albrecht, D. O'Shea, P. Schneeweiss, J. Volz, and A. Rauschenbeutel, Nanophotonic optical isolator controlled by the internal state of cold atoms, Phys. Rev. X **5**, 041036 (2015).

[21] L. Fan, L. T. Varghese, J. Wang, Y. Xuan, A. M. Weiner, and M. Qi, Silicon optical diode with 40 dB nonreciprocal transmission, Opt. Lett. **38**, 1259 (2013).

[22] P. Lodahl, S. Mahmoodian, S. Stobbe, A. Rauschenbeutel, P. Schneeweiss, J. Volz, H. Pichler, and P. Zoller, Chiral quantum optics, Nature (London) **541**, 473 (2017).

[23] T. Nomura, X.-X. Zhang, R. Takagi, K. Karube, A. Kikkawa, Y. Taguchi, Y. Tokura, S. Zherlitsyn, Y. Kohama, and S. Seki, Nonreciprocal phonon propagation in a metallic chiral magnet, Phys. Rev. Lett. **130**, 176301 (2023).

[24] X. Zeng, P. S. J. Russell, C. Wolff, M. H. Frosz, G. K. Wong, and B. Stiller, Nonreciprocal vortex isolator via topology-selective stimulated Brillouin scattering, Sci. Adv. **8**, eabq6064 (2022).

[25] H. Wu, J. Tang, M. Chen, M. Xiao, F. Nori, K. Xia, and Y. Lu, A passive bias-free ultrabroadband optical isolator based on unidirectional self-induced transparency, arXiv:2212.02347 (2022).

[26] K. Xia, F. Nori, and M. Xiao, Cavity-free optical isolators and circulators using a chiral cross-Kerr nonlinearity, Phys. Rev. Lett. **121**, 203602 (2018).

[27] J.-S. Tang, W. Nie, L. Tang, M. Chen, X. Su, Y. Lu, F. Nori, and K. Xia, Nonreciprocal single-photon band structure, Phys. Rev. Lett. **128**, 203602 (2022).

[28] B. Peng, Ş. K. Özdemir, M.Liertzer, W. Chen, J. Kramer, H. Yılmaz, J. Wiersig, S. Rotter, and L. Yang, Chiral modes and directional lasing at exceptional points, Proc. Natl. Acad. Sci. **113**, 6845 (2016).

[29] M. Peng, H. Zhang, Q. Zhang, T.-X. Lu, I. M. Mirza, and H. Jing, Nonreciprocal slow or fast light in anti-$\mathcal{PT}$-symmetric optomechanics, Phys. Rev. A **107**, 033507 (2023).

[30] W. Chen, D. Leykam, Y. Chong, and L. Yang, Nonreciprocity in synthetic photonic materials with nonlinearity, MRS Bull. **43**, 443 (2018).

[31] B. Peng, Ş. K. Özdemir, F. Lei, F. Monifi, M. Gianfreda, G. L. Long, S. Fan, F. Nori, C. M. Bender, and L. Yang, Parity-time-symmetric whispering-gallery microcavities, Nat. Phys. **10**, 394 (2014).

[32] L. Shao, W. Mao, S. Maity, N. Sinclair, Y. Hu, L. Yang, and M. Lončar, Non-reciprocal transmission of microwave acoustic waves in nonlinear parity-time symmetric resonators, Nat. Electron. **3**, 267 (2020).

[33] S. Maayani, R. Dahan, Y. Kligerman, E. Moses, A. U. Hassan, H. Jing, F. Nori, D. N. Christodoulides, and T. Carmon, Flying couplers above spinning resonators generate irreversible refraction, Nature (London) **558**, 569 (2018).

[34] B. Li, Ş. K. Özdemir, X.-W. Xu, L. Zhang, L.-M. Kuang, and H. Jing, Nonreciprocal optical solitons in a spinning Kerr resonator, Phys. Rev. A **103**, 053522 (2021).

[35] D.-W. Zhang, L.-L. Zheng, C. You, C.-S. Hu, Y. Wu, and X.-Y. Lü, Nonreciprocal chaos in a spinning optomechanical resonator, Phys. Rev. A **104**, 033522 (2021).

[36] H. Jing, H. Lü, Ş. K. Özdemir, T. Carmon, and F. Nori, Nanoparticle sensing with a spinning resonator, Optica **5**, 1424 (2018).

[37] H. Zhang, R. Huang, S.-D. Zhang, Y. Li, C.-W. Qiu, F. Nori, and H. Jing, Breaking anti-PT symmetry by spinning a resonator, Nano Lett. **20**, 7594 (2020).

[38] Y.-F. Jiao, S.-D. Zhang, Y.-L. Zhang, A. Miranowicz, L.-M. Kuang, and H. Jing, Nonreciprocal optomechanical entanglement against backscattering losses, Phys. Rev. Lett. **125**, 143605 (2020).

[39] Y.-F. Jiao, J.-X. Liu, Y. Li, R. Yang, L.-M. Kuang, and H. Jing, Nonreciprocal enhancement of remote entanglement between nonidentical mechanical oscillators, Phys. Rev. Appl. **18**, 064008 (2022).

[40] Y. Xiang, Y. Zuo, X.-W. Xu, R. Huang, and H. Jing, Switching classical and quantum nonreciprocities with a single spinning resonator, Phys. Rev. A **108**, 043702 (2023).

[41] R. Huang, A. Miranowicz, J.-Q. Liao, F. Nori, and H. Jing, Nonreciprocal photon blockade, Phys. Rev. Lett. **121**, 153601 (2018).

[42] B. Li, R. Huang, X. Xu, A. Miranowicz, and H. Jing, Nonreciprocal unconventional photon blockade in a spinning optomechanical system, Photon. Res. **7**, 630 (2019).

[43] Y.-W. Jing, H.-Q. Shi, and X.-W. Xu, Nonreciprocal photon blockade and directional amplification in a spinning resonator coupled to a two-level atom, Phys. Rev. A **104**, 033707 (2021).

[44] X.-Y. Yao, H. Ali, F.-L. Li, and P.-B. Li, Nonreciprocal phonon blockade in a spinning acoustic ring cavity coupled to a two-level system, Phys. Rev. Appl. **17**, 054004 (2022).

[45] N. Yuan, S. He, S.-Y. Li, N. Wang, and A.-D. Zhu, Optical noise-resistant nonreciprocal phonon blockade in a spinning optomechanical resonator, Opt. Express **31**, 20160 (2023).

[46] L. Jin, J.-X. Peng, Q.-Z. Yuan, and X.-L. Feng, Macroscopic quantum coherence in a spinning optomechanical system, Opt. Express **29**, 41191 (2021).

[47] Y. Liu, J. Cheng, H. Wang, and X. Yi, Nonreciprocal photon blockade in a spinning optomechanical system with nonreciprocal coupling, Opt. Express **31**, 12847 (2023).

[48] K. Ullah, H. Jing, and F. Saif, Multiple electromechanically-induced-transparency windows and Fano resonances in hybrid nano-electro-optomechanics, Phys. Rev. A **97**, 033812 (2018).

[49] H.-t. Tan and G.-X. Li, Multicolor quadripartite entanglement from an optomechanical cavity, Phys. Rev. A **84**, 024301 (2011).

[50] G. Pan, R. Xiao, H. Chen, and J. Gao, Multicolor optomechanically induced transparency in a distant nano-electro-optomechanical system assisted by two-level atomic ensemble, Laser Phys. **31**, 065202 (2021).

[51] R.-J. Xiao, G.-X. Pan, and L. Zhou, Analog multicolor electromagnetically induced transparency in multimode quadratic coupling quantum optomechanics, J. Opt. Soc. Am. B **32**, 1399 (2015).

[52] A. Krasnok and A. Alù, Active nanophotonics, Proc. IEEE **108**, 628 (2020).

[53] Y. He, Z. Su, F. Cao, Z. Cao, Y. Liu, C. Zhao, G. Weng, X. Hu, J. Tao, J. Chu, H. Akiyama, and S. Chen, Lasing properties and carrier dynamics of $CsPbBr_3$ perovskite nanocrystal vertical-cavity surface-emitting laser, Nanophotonics **12**, 2133 (2023).

[54] K. Liao, Y. Zhong, Z. Du, G. Liu, C. Li, X. Wu, C. Deng, C. Lu, X. Wang, C. T. Chan *et al.*, On-chip integrated exceptional surface microlaser, Sci. Adv. **9**, eadf3470 (2023).

[55] F. Lohof, A. Steinhoff, M. Florian, M. Lorke, D. Erben, F. Jahnke, and C. Gies, Prospects and limitations of transition metal dichalcogenide laser gain materials, Nano Lett. **19**, 210 (2019).

[56] V. Klimov, A. Mikhailovsky, S. Xu, A. Malko, J. Hollingsworth, C. Leatherdale, H.-J. Eisler, and M. Bawendi, Optical gain and stimulated emission in nanocrystal quantum dots, Science **290**, 314 (2000).

[57] S.-S. Gu, Y.-Q. Xu, R. Wu, S.-L. Jiang, S.-K. Ye, T. Lin, B.-C. Wang, H.-O. Li, G. Cao, and G.-P. Guo, Gain of a high-impedance cavity coupled to strongly driven semiconductor quantum dots, Phys. Rev. Appl. **19**, 054020 (2023).

[58] Y. Liu, Z. Qiu, X. Ji, A. Lukashchuk, J. He, J. Riemensberger, M. Hafermann, R. N. Wang, J. Liu, C. Ronning *et al.*, A photonic integrated circuit-based erbium-doped amplifier, Science **376**, 1309 (2022).

[59] H. Hodaei, M.-A. Miri, M. Heinrich, D. N. Christodoulides, and M. Khajavikhan, Parity-time-symmetric microring lasers, Science **346**, 975 (2014).

[60] L. He, Ş. K. Özdemir, and L. Yang, Whispering gallery microcavity lasers, Laser Photonics Rev. **7**, 60 (2013).

[61] H. Jing, Ş. K. Özdemir, X.-Y. Lü, J. Zhang, L. Yang, and F. Nori, $\mathcal{PT}$-symmetric phonon laser, Phys. Rev. Lett. **113**, 053604 (2014).

[62] H. Jing, Ş. K. Özdemir, Z. Geng, J. Zhang, X.-Y. Lü, B. Peng, L. Yang, and F. Nori, Optomechanically-induced transparency in parity-time-symmetric microresonators, Sci. Rep. **5**, 9663 (2015).

[63] S. Baek, S.-H. Park, D. Oh, K. Lee, S. Lee, H. Lim, T. Ha, H.-S. Park, S. Zhang, Y. Lan, B. Min, and T.-T. Kin, Non-Hermitian chiral degeneracy of gated graphene metasurfaces, Light Sci. Appl. **12**, 87 (2023).

[64] Y. G. N. Liu, Y. Wei, O. Hemmatyar, G. G. Pyrialakos, P. S. Jung, D. N. Christodoulides, and M. Khajavikhan, Complex

skin modes in non-Hermitian coupled laser arrays, Light Sci. Appl. **11**, 336 (2022).
[65] L. Wang, A. Kuzmich, and A. Dogariu, Gain-assisted superluminal light propagation, Nature (London) **406**, 277 (2000).
[66] T. Oishi and M. Tomita, Inverted coupled-resonator-induced transparency, Phys. Rev. A **88**, 013813 (2013).
[67] Y. Jiao, H. Lü, J. Qian, Y. Li, and H. Jing, Nonlinear optomechanics with gain and loss: Amplifying higher-order sideband and group delay, New J. Phys. **18**, 083034 (2016).
[68] Y. Ke, J. Huang, W. Liu, Y. Kivshar, and C. Lee, Topological inverse band theory in waveguide quantum electrodynamics, Phys. Rev. Lett. **131**, 103604 (2023).
[69] B. He, L. Yang, and M. Xiao, Dynamical phonon laser in coupled active-passive microresonators, Phys. Rev. A **94**, 031802 (2016)(R).
[70] X.-Y. Lü, H. Jing, J.-Y. Ma, and Y. Wu, $\mathcal{PT}$-symmetry-breaking chaos in optomechanics, Phys. Rev. Lett. **114**, 253601 (2015).
[71] Ş. K. Özdemir, S. Rotter, F. Nori, and L. Yang, Parity-time symmetry and exceptional points in photonics, Nat. Mater. **18**, 783 (2019).
[72] J. Zhang, B. Peng, Ş. K. Özdemir, Y.-X. Liu, H. Jing, X.-Y. Lü, Y.-L. Liu, L. Yang, and F. Nori, Giant nonlinearity via breaking parity-time symmetry: A route to low-threshold phonon diodes, Phys. Rev. B **92**, 115407 (2015).
[73] L. Chang, X. Jiang, S. Hua, C. Yang, J. Wen, L. Jiang, G. Li, G. Wang, and M. Xiao, Parity-time symmetry and variable optical isolation in active–passive-coupled microresonators, Nat. Photonics **8**, 524 (2014).
[74] J. Ma, J. Wen, S. Ding, S. Li, Y. Hu, X. Jiang, L. Jiang, and M. Xiao, Chip-based optical isolator and nonreciprocal parity-time symmetry induced by stimulated Brillouin scattering, Laser Photonics Rev. **14**, 1900278 (2020).
[75] T. Kuang, R. Huang, W. Xiong, Y. Zuo, X. Han, F. Nori, C.-W. Qiu, H. Luo, H. Jing, and G. Xiao, Nonlinear multi-frequency phonon lasers with active levitated optomechanics, Nat. Phys. **19**, 414 (2023).
[76] W. Yang, S. A. Gerke, K. W. Ng, Y. Rao, C. Chase, and C. J. Chang-Hasnain, Laser optomechanics, Sci. Rep. **5**, 1 (2015).
[77] T. Czerniuk, C. Brüggemann, J. Tepper, S. Brodbeck, C. Schneider, M. Kamp, S. Höfling, B. A. Glavin, D. R. Yakovlev, A. V. Akimov *et al.*, Lasing from active optomechanical resonators, Nat. Commun. **5**, 4038 (2014).
[78] Z.-P. Liu, J. Zhang, Ş. K. Özdemir, B. Peng, H. Jing, X.-Y. Lü, C.-W. Li, L. Yang, F. Nori, and Y. X. Liu, Metrology with $\mathcal{PT}$-symmetric cavities: Enhanced sensitivity near the $\mathcal{PT}$-phase transition, Phys. Rev. Lett. **117**, 110802 (2016).
[79] H. Guo, M. Karpov, E. Lucas, A. Kordts, M. H. Pfeiffer, V. Brasch, G. Lihachev, V. E. Lobanov, M. L. Gorodetsky, and T. J. Kippenberg, Universal dynamics and deterministic switching of dissipative Kerr solitons in optical microresonators, Nat. Phys. **13**, 94 (2017).
[80] A. H. Safavi-Naeini, T. M. Alegre, J. Chan, M. Eichenfield, M. Winger, Q. Lin, J. T. Hill, D. E. Chang, and O. Painter, Electromagnetically induced transparency and slow light with optomechanics, Nature (London) **472**, 69 (2011).
[81] S. Weis, R. Rivière, S. Deléglise, E. Gavartin, O. Arcizet, A. Schliesser, and T. J. Kippenberg, Optomechanically induced transparency, Science **330**, 1520 (2010).
[82] D.-K. Zhang, X.-Q. Luo, Y.-P. Wang, T.-F. Li, and J.-Q. You, Observation of the exceptional point in cavity magnon-polaritons, Nat. Commun. **8**, 1368 (2017).
[83] G.-Q. Zhang and J.-Q. You, Higher-order exceptional point in a cavity magnonics system, Phys. Rev. B **99**, 054404 (2019).
[84] Y. Wang, H.-L. Zhang, J.-L. Wu, J. Song, K. Yang, W. Qin, H. Jing, and L.-M. Kuang, Quantum parametric amplification of phonon-mediated magnon-spin interaction, Sci. China: Phys. Mech. Astron. **66**, 1869 (2023).
[85] W. Zhao, S.-D. Zhang, A. Miranowicz, and H. Jing, Weak-force sensing with squeezed optomechanics, Sci. China: Phys. Mech. Astron. **63**, 1869 (2019).
[86] G. B. Malykin, The Sagnac effect: Correct and incorrect explanations, Phys.-Usp. **43**, 1229 (2000).
[87] X. Mao, H. Yang, D. Long, M. Wang, P.-Y. Wen, Y.-Q. Hu, B.-Y. Wang, G.-Q. Li, J.-C. Gao, and G.-L. Long, Experimental demonstration of mode-matching and Sagnac effect in a millimeter-scale wedged resonator gyroscope, Photon. Res. **10**, 2115 (2022).
[88] Z. Yang, Y. Cheng, N. Wang, Y. Chen, and S. Wang, Nonreciprocal light propagation induced by a subwavelength spinning cylinder, Opt. Express **30**, 27993 (2022).
[89] J. Burns, O. Root, H. Jing, and I. M. Mirza, Engineering optomechanically induced transparency by coupling a qubit to a spinning resonator, J. Opt. Soc. Am. B **40**, 958 (2023).
[90] Y. Jiang, S. Maayani, T. Carmon, F. Nori, and H. Jing, Nonreciprocal phonon laser, Phys. Rev. Appl. **10**, 064037 (2018).
[91] H. Shi, Z. Xiong, W. Chen, J. Xu, S. Wang, and Y. Chen, Gauge-field description of Sagnac frequency shift and mode hybridization in a rotating cavity, Opt. Express **27**, 28114 (2019).
[92] S. Davuluri and S. Zhu, Controlling optomechanically induced transparency through rotation, Europhys. Lett. **112**, 64002 (2015).
[93] T.-X. Lu, X. Xiao, L.-S. Chen, Q. Zhang, and H. Jing, Magnon-squeezing-enhanced slow light and second-order sideband in cavity magnomechanics, Phys. Rev. A **107**, 063714 (2023).
[94] H. Zhang, F. Saif, Y. Jiao, and H. Jing, Loss-induced transparency in optomechanics, Opt. Express **26**, 25199 (2018).
[95] C. W. Gardiner and M. J. Collett, Input and output in damped quantum systems: Quantum stochastic differential equations and the master equation, Phys. Rev. A **31**, 3761 (1985).
[96] Y.-J. Jiang, X.-D. Zhao, S.-Q. Xia, C.-J. Yang, W.-M. Liu, and Z.-L. Zhu, Nonlinear optomechanically induced transparency in a spinning Kerr resonator, Chin. Phys. Lett. **39**, 124202 (2022).
[97] H. Lü, Y. Jiang, Y.-Z. Wang, and H. Jing, Optomechanically induced transparency in a spinning resonator, Photon. Res. **5**, 367 (2017).
[98] H. Xiong, L.-G. Si, A.-S. Zheng, X. Yang, and Y. Wu, Higher-order sidebands in optomechanically induced transparency, Phys. Rev. A **86**, 013815 (2012).
[99] M.-A. Lemonde, N. Didier, and A. A. Clerk, Nonlinear interaction effects in a strongly driven optomechanical cavity, Phys. Rev. Lett. **111**, 053602 (2013).
[100] Y.-C. Liu, Y.-F. Xiao, Y.-L. Chen, X.-C. Yu, and Q. Gong, Parametric down-conversion and polariton pair generation in optomechanical systems, Phys. Rev. Lett. **111**, 083601 (2013).

[101] A. Kronwald and F. Marquardt, Optomechanically induced transparency in the nonlinear quantum regime, Phys. Rev. Lett. **111**, 133601 (2013).

[102] Y.-F. Jiao, T.-X. Lu, and H. Jing, Optomechanical second-order sidebands and group delays in a Kerr resonator, Phys. Rev. A **97**, 013843 (2018).

[103] J. Li, J. Li, Q. Xiao, and Y. Wu, Giant enhancement of optical high-order sideband generation and their control in a dimer of two cavities with gain and loss, Phys. Rev. A **93**, 063814 (2016).

[104] H. Suzuki, E. Brown, and R. Sterling, Nonlinear dynamics of an optomechanical system with a coherent mechanical pump: Second-order sideband generation, Phys. Rev. A **92**, 033823 (2015).

[105] A. A. Reynoso, G. Usaj, D. L. Chafatinos, F. Mangussi, A. E. Bruchhausen, A. S. Kuznetsov, K. Biermann, P. V. Santos, and A. Fainstein, Optomechanical parametric oscillation of a quantum light-fluid lattice, Phys. Rev. B **105**, 195310 (2022).

[106] X. Wang, K.-W. Huang, and H. Xiong, Nonreciprocal sideband responses in a spinning microwave magnomechanical system, Opt. Express **31**, 5492 (2023).

[107] W.-A. Li, G.-Y. Huang, J.-P. Chen, and Y. Chen, Nonreciprocal enhancement of optomechanical second-order sidebands in a spinning resonator, Phys. Rev. A **102**, 033526 (2020).

[108] M. Wang, C. Kong, Z.-Y. Sun, D. Zhang, Y.-Y. Wu, and L.-L. Zheng, Nonreciprocal high-order sidebands induced by magnon Kerr nonlinearity, Phys. Rev. A **104**, 033708 (2021).

[109] Z. Shen, C.-H. Dong, Y. Chen, Y.-F. Xiao, F.-W. Sun, and G.-C. Guo, Compensation of the Kerr effect for transient optomechanically induced transparency in a silica microsphere, Opt. Lett. **41**, 1249 (2016).

[110] Y. C. Liu, X. Luan, H.-K. Li, Q. Gong, C.-W. Wong, and Y.-F. Xiao, Coherent polariton dynamics in coupled highly dissipative cavities, Phys. Rev. Lett. **112**, 213602 (2014).

[111] Ş. K. Özdemir, J. Zhu, X. Yang, B. Peng, H. Yilmaz, L. He, F. Monifi, S.-H. Huang, G. Long, and L. Yang, Highly sensitive detection of nanoparticles with a self-referenced and self-heterodyned whispering-gallery Raman microlaser, Proc. Natl. Acad. Sci. **111**, E3836 (2014).

[112] H. Zhang, M. Peng, X.-W. Xu, and H. Jing, Anti-symmetric Kerr gyroscope, Chin. Phys. B **31**, 014215 (2022).

[113] J.-Q. Zhang, J.-X. Liu, H.-L. Zhang, Z.-R. Gong, S. Zhang, L.-L. Yan, S.-L. Su, H. Jing, and M. Feng, Topological optomechanical amplifier in synthetic PT-symmetry, Nanophotonics **11**, 1149 (2022).